A NOVEL APPROACH ON ENABLING STACKED DIE INTEGRATION TECHNOLOGY IN OVERMOLDED PACKAGES USING CONDUCTIVE DIE ATTACH FILM

Marty Lorgino D. Pulutan
Norman Y. Lanuza
Patrisha Louise M. Reyes

Backend Technologies
Ampleon Philippines, Inc., Light Industry & Science Park I, Brgy. Diezmo, Cabuyao City, Laguna
marty.lorgino.pulutan@ampleon.com

ABSTRACT

The study presents the first comprehensive evaluation of conductive die attach films (CDAFs) in stacked-die RF power semiconductor packages, addressing a critical gap in both literature and industrial application. Among various die stacking configurations, the pyramid layout was selected based on mechanical risk assessment for ultra-thin dies. Three candidate CDAF materials were initially evaluated through a paper-based assessment with CDAF Z subsequently dropped from further evaluation due to the risks associated with the 60% Cu content in the formulation. Two CDAF candidates were extensively characterized through thermal, mechanical, morphological, and electrical analyses including Differential Scanning Calorimetry (DSC), Thermogravimetric Analysis (TGA), SEM imaging, and finite element modeling. Experimental results demonstrate that both materials exhibit robust adhesion, mechanical integrity under thermal cycling, and process compatibility. Notably, CDAF Y showed superior flow control, reduced die tilt and more consistent capacitance performance across 1000 thermal cycles indicating enhanced adhesion stability on ceramic interfaces. Additionally, stacked-die configurations using CDAF achieved nearly 50% reduction in capacitance which confirms the potential to simultaneously address parasitic and thermal limitations in RF applications. The study proposes a practical loop height design rule and validates CDAF as a viable material for stacked die application in RF power packaging.

1. 0 INTRODUCTION

The rapid advancement of radio-frequency (RF) power semiconductors is transforming the landscape of broadband communication and emerging domains such as 5G and beyond. The challenges of meeting the growing demands for higher power density, enhanced efficiency and complex miniaturization require innovative packaging materials that can ensure thermal, mechanical, and electrical performance under high-frequency operating conditions. A critical yet underexplored enabler of next-generation stacked RF power packaging is the CDAF. In contrast to conventional die attach materials, CDAF provides not only high thermal conductivity and low voiding but also electrically conductive pathways which is a critical requirement for efficient signal transmission in high-frequency RF applications. Moreover, CDAF offers the potential for improved bonding uniformity and mechanical reliability in ultra-thin die configurations where thermal stress and signal integrity pose significant design challenges.

While prior studies have examined various die attach techniques and materials for thermal and mechanical performance, there is currently no published research or known industry implementation that utilizes CDAF specifically for stacked die RF power packages. Benchmarking of commercial RF power modules confirms the absence of CDAF adoption in existing product lines, making this study the first of its kind to explore the feasibility and benefits of integrating CDAF into vertically stacked RF semiconductor architectures. In addition to its mechanical and electrical roles, the study uniquely investigates how CDAF can be engineered to contribute to in-package capacitance optimization—enhancing power integrity and reducing parasitic effects in high-frequency environments. The integration of capacitor-enhancing materials within the die attach layer represents a novel packaging strategy that addresses both thermal and electrical constraints simultaneously. The study presents a novel evaluation of CDAF integration for stacked die RF power devices, addressing a critical gap in research and industry to advance compact, efficient, and thermally robust RF packaging.

2. 0 REVIEW OF RELATED WORK

The incessant miniaturization of semiconductor devices has brought forth unique challenges in die-level packaging and material performance particularly in ultrathin die applications. As Si die thicknesses shrink below 100 µm, mechanical robustness becomes increasingly compromised due to phenomena such as bowing, warpage, and subsurface damage. Such deformation mechanisms drastically reduce the mechanical strength of the die and elevate the risk of fracture during assembly processes such as die attach and wirebonding[1]. One key approach to mitigate the risks is to select appropriate material with optimum properties particularly the elastic modulus. Unger et al.[2] demonstrated through experimental and numerical studies that bonding materials with reduced modulus values can attenuate stress concentrations during ultrasonic wirebonding thereby decreasing the likelihood of die cracking. However, they also cautioned that an excessively low modulus may undermine mechanical stability and bond strength, highlighting the importance of tuning material properties to balance compliance with structural integrity. In addition to modulus, filler morphology and distribution play a critical role in die attach material selection and optimization. The particle size distribution (PSD) of conductive fillers must be tightly controlled as larger particles tend to reduce conformability on complex bonding surfaces, thereby degrading interfacial adhesion and increasing the likelihood of contact discontinuities[3].

Meanwhile, curing profile dictates the adhesion strength of bonding materials like CDAF. Carbas et al.[4] demonstrated that curing near the fully cross-linked glass transition temperature (Tg∞) enhances cross-link density and mechanical strength but exceeding beyond can trigger polymer degradation ultimately reducing both Tg and structural performance. Such findings underscore the importance of tailoring cure conditions to maximize cross-linking while avoiding thermal damage.

Failure analysis studies by Ansys further highlight the importance of controlled adhesive application. Excessive material or bonding force can result in excessive flow-out beyond the die perimeter, potentially causing electrical shorting by encroaching upon adjacent terminals or pads particularly in fine-pitch configurations[5]. Emerging material solutions such as Die Attach Films (DAFs) offer substantial benefits in addressing such challenges. The integration of DAFs has shown promise in maintaining consistent bondline thickness (BLT) and reducing die tilt—both critical to minimizing delamination and improving die planarity during encapsulation. DAFs also limit collet contamination and void formation due to their controlled thickness and predictable curing behavior, improving both reliability and manufacturability[6].

Collectively, the reported studies establish a comprehensive framework for optimizing die attach and bonding systems in advanced packaging. Material selection, processing conditions, and structural integrity must be carefully co-optimized to accommodate the mechanical sensitivity of ultrathin dies especially for stacked-die application.

3.0 METHODOLOGY

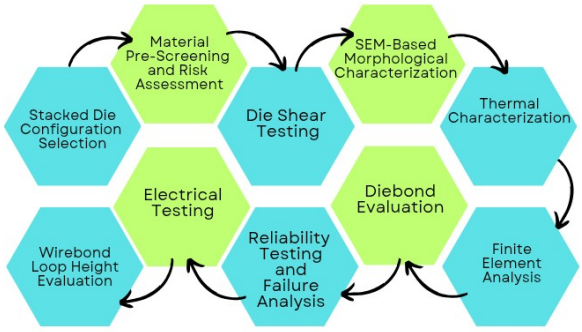

Fig. 1. Experimental Workflow for the Development of Stacked Die Configuration Using Conductive Die Attach Film.

Three CDAF candidates were pre-screened through material property comparisons from technical data sheets (TDS) and die shear testing per MIL-STD-883 to assess adhesion strength. CDAF X and Y underwent SEM-based morphological analysis and PSD quantification using Fiji, while DSC and TGA characterized thermal behavior. Finite Element Analysis (FEA) in Ansys simulated interfacial stresses and safety factors. Die bond workability was assessed through flow-out, tilt, and placement accuracy, supported by ANOVA and PpK analysis. Reliability was evaluated via SAT and SEM cross-sectioning after 1000 thermal cycles, and electrical performance was verified through DC capacitance testing. Wire bond reliability was addressed by establishing loop height design rules using a geometric model.

4.0 RESULTS AND DISCUSSION

4.1 Selection of Stacked Die Configuration

Three configurations were considered: pyramid, stair, and T-mode. In the pyramid layout, a smaller daughter die is stacked atop a larger mother die, forming a tapered profile. The stair configuration offsets the

daughter die laterally, creating a step-like structure. In the T-mode, the larger daughter die is placed perpendicularly atop the smaller mother die, forming a T-shaped stack.

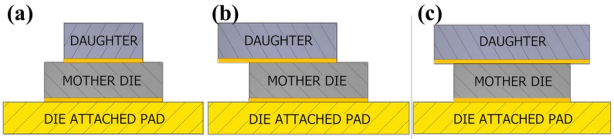

Fig. 2. Different Stacked Die Configuration Variants Considered in the Study – Pyramid (a), Stair (b) and T-Mode (c).

Considering a risk assessment based on the ultrathin die thickness of approximately 60µm and the current capabilities of the manufacturing process, the risk of die cracking is deemed high[1]. Consequently, both the stair and T-mode configurations are not viable options. As a result, the pyramid configuration is selected as the optimal choice for further development.

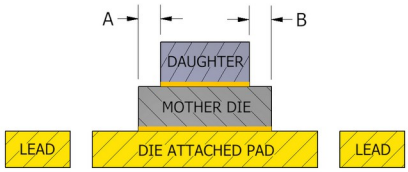

Fig. 3. Illustration of Daughter-to-Mother Die Alignment and Lateral Offset in a Pyramid Stacked Die Configuration.

Two pyramid-stacked die configurations were evaluated based on risk. The first variant would use a smaller daughter die than the mother die (Fig. 3), while the second would use identical die sizes. A critical reliability risk is electrical shorting between the CDAF and the mother die's attach layer or die pad, typically caused by CDAF overflow or conductive slivers. To mitigate this, a minimum edge margin of 65 µm is recommended. While resizing increases lead time, using identical dies demands high die placement accuracy to prevent lateral misalignment which can lead to overhang, stair-step profiles, and mechanical cracking. Due to the higher cost and process risk of the latter, the smaller daughter die configuration was selected for further evaluation in die attach material screening.

4.2 Paper Study: Material Property Comparison and Risk Assessment

Given the absence of existing studies or industry applications of CDAF in stacked die configurations, material selection should begin with a comparative analysis of key properties and associated risks. Table 1 summarizes the relevant properties of the three CDAF materials obtained from TDS.

Table 1. Key Material Properties of the Three CDAF Candidates.

Properties	CDAF X	CDAF Y	CDAF Z
Thickness (µm)	30	15	25
Volume Resistivity (Ω·cm)	0.0007	0.0004	0.008
Thermal Conductivity (W/mK)	2.3	1.8	1.0
Modulus (N/mm²)	5400	6530	3000
CTE 1 (ppm/K)	48	75	75
CTE 2 (ppm/K)	119	274	320
Tg (ºC)	15	5	-5

The proposed stacked die configuration aims to enhance capacitance by enabling electrical and thermal coupling between the mother and daughter capacitors, favoring materials with low volume resistivity and high thermal conductivity. CDAF X and Y exhibit significantly lower volume resistivity than CDAF Z, supporting more efficient electrical interconnection. Conversely, CDAF Z is expected to offer improved thermal dissipation due to its higher thermal conductivity. The elastic modulus of the three materials varies and must be optimized—lower modulus reduces die cracking risk particularly for thin dies, but excessively low values may compromise structural integrity during ultrasonic wirebonding on the daughter die. All three materials exhibit low glass transition temperatures (Tg), suggesting operation within CTE 2 during assembly and testing. CDAF X demonstrates the closest CTE match to Si (2.6–3.0 ppm/K), minimizing interfacial stress and reducing delamination risk under thermal cycling.

Currently, no literature establishes whether CDAF can reliably adhere to the ceramic regions on the mother die active side under cyclic loading and humidity stress. As such, die shear strength and material composition are critical indicators for assessing adhesion and long-term reliability. Shear testing was conducted in accordance with MIL-STD-883, Method 2019, targeting 50% of the CDAF thickness and applying a minimum force specification of 2.5 kgF based on die dimensions.[11].

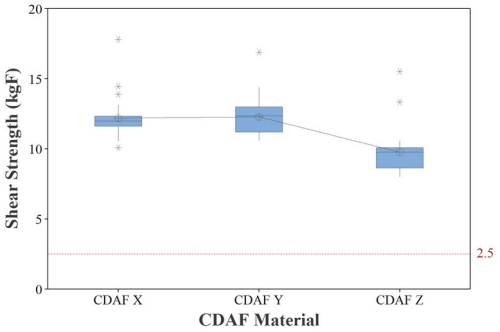

Fig. 4. Shear Strength Distribution of Various CDAF Materials with Failure Threshold.

Tukey pairwise comparison revealed that CDAF Z exhibited significantly lower adhesion strength than CDAF X and Y. Hsu's Multiple Comparisons with the Best (MCB) further confirmed that CDAF X and Y had comparable adhesion performance, both superior to CDAF Z. Such differences are likely due to material composition—CDAF X and Y contain around 30% proprietary resin, while CDAF Z contains only 20%. Additionally, CDAF Z's high Cu content (~60%) increases susceptibility to oxidation under high-humidity conditions due to moisture ingress via micro-delaminations. As a result, CDAF X and Y were selected for further characterization.

4.3 *Material Characterization: Differences in Surface Morphology, Topology and Thermal Behavior*

Few CDAF X and Y samples were mounted on wafers and diced into 4.00 × 0.80 mm and 3.85 × 0.65 mm, matching the die dimensions of the OMP device carrier. Samples were cured per their respective TDS-specified profiles and imaged using SEM at 15 keV to obtain high-resolution microstructural characterization.

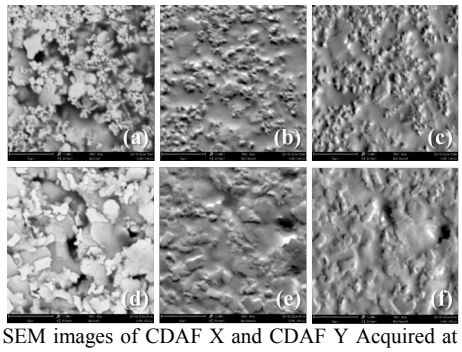

Fig. 5. SEM images of CDAF X and CDAF Y Acquired at 10,000× Magnification Using Different Detectors: (a–c) CDAF X imaged with (a) backscattered electron detector (BSD full), (b) topographic detector A (Topo A), and (c) topographic detector B (Topo B); (d–f) CDAF Y imaged with (d) BSD full, (e) Topo A, and (f) Topo B.

Comparative microstructural analysis reveals a higher prevalence of larger Ag flake fillers in CDAF Y whereas CDAF X exhibits a greater density of smaller Ag particles. The presence of larger flakes in CDAF Y may hinder their ability to conform effectively to the surface topology of Si_3N_4 ceramic regions in the die, potentially compromising interfacial contact quality. Such morphological mismatch could lead to discontinuities at the interface thereby diminishing bond integrity due to the formation of non-uniform or poorly adhered contact layers[3].

The thermal behavior and stability of CDAF X and Y were then assessed using DSC and TGA with heat rates of 1, 3, 5 and 10ºC/min.

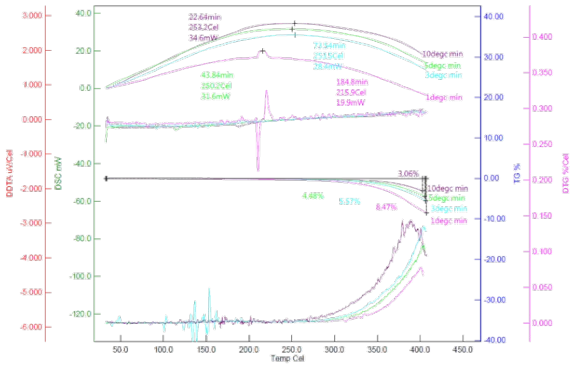

Fig. 6. DSC, TGA and Corresponding Derivative Curves of CDAF Y Obtained at Heating Rates of 1, 3, 5, and 10 °C/min.

The peak curing temperatures were identified at approximately 240 °C for CDAF X (see Fig. 15 in Appendix) and 250 °C for CDAF Y corresponding to the maximum exothermic reactions associated with cross-linking during the thermosetting process. The thermal degradation of both materials begins near 300 °C as indicated by a distinct exothermic event accompanied by thermal decomposition confirmed through TGA peaks. The gap between the peak curing temperature and the onset of degradation defines a favorable thermal processing window. Increasing the curing temperature toward the exothermic peak enhances the extent of cross-linking which can improve adhesion and mechanical performance. However, temperatures approaching the degradation threshold must be avoided to prevent material decomposition and associated deterioration in functional properties[4]. Therefore, the curing protocol should be precisely controlled to achieve optimal material performance without compromising structural or chemical stability.

Analysis of DSC thermograms under varying heating rates revealed negligible shifts in the curing peak temperatures for both materials. The absence of significant thermal lag indicates that the curing kinetics are largely independent of the applied heating rate. Uniform cross-linking behavior suggests that both

CDAF X and Y possess stable polymerization mechanisms and consistent thermal response characteristics regardless of thermal ramp rate. The insensitivity of phase transitions to changes in thermal input further confirms the robustness of these materials under different processing conditions.

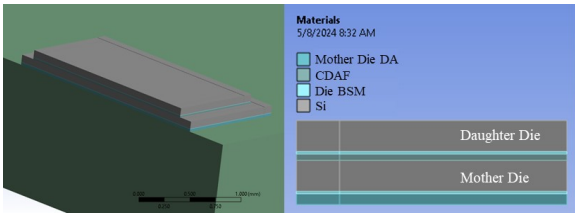

Fig. 7. Finite Element Model Showing Material Composition in Multi-Die Package.

FEA simulations were conducted using Ansys software to evaluate the interfacial stress and safety factor of two CDAF materials. The simulation incorporated the material constituents of the package, including a Cu heatsink (Young's modulus: 131 GPa, Poisson's ratio: 0.34), a high-adhesion epoxy molding compound (EMC) (Young's modulus: 24.5 GPa, Poisson's ratio: 0.35), and a die attach layer between the mother die and heatsink (Young's modulus: 8 GPa, Poisson's ratio: 0.35). The simulation results reveal that the safety factors for CDAF X and CDAF Y are relatively similar, calculated as 2.15 and 2.21 respectively. Both values are well above the critical threshold of 1.0 indicating that the materials possess sufficient mechanical robustness to endure the interfacial stresses encountered during thermal and mechanical loading. A closer examination of the interfacial stress values shows that CDAF Y experiences a slightly higher maximum stress at the interface approximately 37.558 MPa, whereas CDAF X registers a lower stress of 32.673 MPa. The elevated interfacial stress in CDAF Y is hypothesized to stem from its higher Tg, which is approximately 10°C greater than that of CDAF X. A higher Tg typically implies increased material stiffness at elevated temperatures, potentially resulting in greater thermal mismatch-induced stress at the interfaces particularly during thermal cycling or curing processes. Despite the increase in interfacial stress, the safety factor for CDAF Y remains favorable, suggesting that the material's mechanical integrity is not compromised.

Considering both safety factor and interfacial stress together, the performance of CDAF X and Y appears to be largely equivalent from a thermomechanical standpoint. The marginal differences observed are not expected to significantly impact the long-term reliability or structural stability of the package. Consequently, either material could be considered viable depending on additional factors such as processing requirements, cost, or availability. Both CDAF materials advanced to the build validation phase to assess difference in manufacturing process performance and long-term reliability.

4.4 Diebond Workability of CDAF X and Y on Stacked Die Configuration

The die bonding workability of CDAF X and Y was evaluated to assess the feasibility for stacked-die configurations. The objective was to determine compliance with die bonding process requirements and identify which material offers superior processability with lower integration risks.

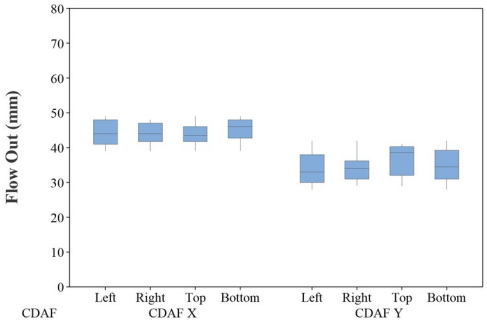

Fig. 8. Comparison of Flow Out Measurements for CDAF X and Y Across Die Edges.

The die attach flow out on all sides of the die were measured and presented in Fig. 8. Based on Fully Nested ANOVA, there is a significant difference between the flow out of between units using CDAF X and Y based on p-value of 0.001 where CDAF X shows significantly larger flow out than CDAF Y signifying lower thixotropic index than CDAF Y. Such observations may imply that the CDAF X material responds more on bonding force and might produce flow out exceeding the prescribed margin of mother and daughter die leading to shorting[5]. Meanwhile, die tilt of the daughter die was measured relative to the mother die for both materials (see Fig. 16 in Appendix).

Although both materials demonstrate die tilt values well below the maximum allowable specification of 30 µm, the improved self-leveling capability of CDAF Y which can be attributed to its increased thickness, is evident based on the results of a one-way ANOVA test which yielded a statistically significant p-value of 0.005. While both materials are within acceptable limits, CDAF Y is preferable due to its superior ability to minimize die tilt, thereby reducing the risk of asymmetric stress distribution and capacitance variation.

Additional die bonding response parameters such as die placement accuracy along the X- and Y-axes as well as the rotational alignment (angular deviation) of the daughter die relative to the mother die were also characterized.

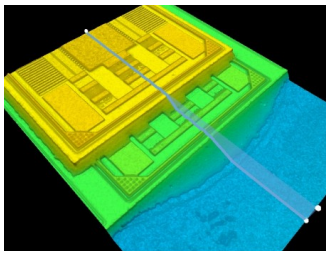

Fig. 9. 3D Optical Profiling Image of Actual Stacked Capacitor Dies Illustrating Lateral Offset.

Utilizing die placement and angular alignment tolerances of ±30 µm and ±0.5° respectively, both materials demonstrated high process fidelity achieving PpK exceeding 1.33. Such results indicate that the existing die bonding process exhibits a high degree of statistical control for both materials, thereby minimizing the likelihood of die misalignment or overhang and the associated risk of mechanical stress-induced die cracking.

4.5 Package Level Evaluation and Reliability Tests

Twenty overmolded package carrier units, each containing four stacked die pairs, were assembled and subjected to thermal cycling from -65 °C to 150 °C. Scanning Acoustic Tomography (SAT) was conducted at key intervals: post-mold cure (PMC), post-preconditioning, and after 500 and 1000 cycles. At each stage, two units underwent destructive analysis. Cross-sections were taken at the longitudinal midpoint of the stacked dies and examined via SEM to assess delamination, voids, or die attach defects.

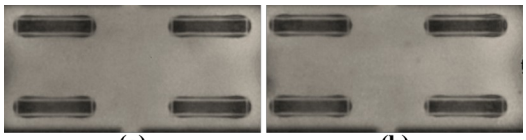

(a) (b)

Fig. 10. SAT Images of CDAF X and Y Post 1000 Cycles of Thermal Cycling.

SAT imaging, gated between the CDAF and the mother die's active side and validated via A-scan, revealed no interfacial delamination across all samples. C-scan images of units with CDAF X and Y showed no high-amplitude contrast regions at PMC and after 1000 thermal cycles, indicating robust adhesion and mechanical integrity under thermomechanical stress. SEM cross-sections at 1000×, along with high-resolution BSD and SED imaging at 10,000×, confirmed the absence of voids, cracks, or separations at the interface.

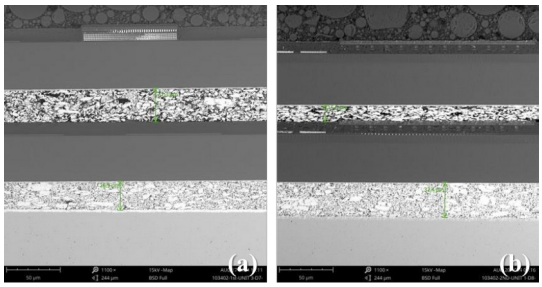

Fig. 11. Cross-section images of units using (a) CDAF X and (b) CDAF Y obtained using SEM at 1000× magnification.

The measured bondline thickness (BLT) of cured CDAF X and Y ranged from 30.1–31.6 µm and 15.2–17.7 µm, respectively, across units from PMC to post-1000 thermal cycles. An F-test for equality of variances revealed significantly lower BLT variance for CDAF X, indicating reduced die tilt. Such findings support the self-leveling behavior of thicker CDAF in compensating for non-uniform mother die planarity[6]. PSD analysis of SEM cross-sections, measured via Fiji software, is shown in Fig. 12.

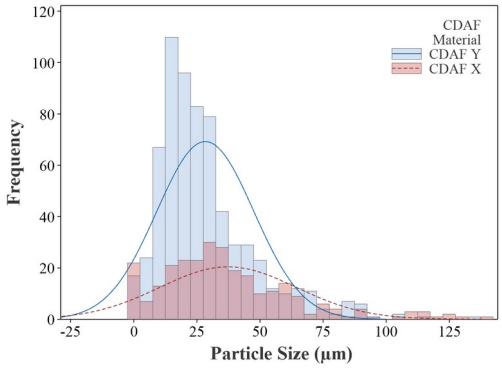

Fig. 12. PSD of CDAF X and Y obtained using Fiji software. Capacitance Trends of Cap and CDAF Materials Across TMCL Readpoints.

The PSD results are consistent with observations from SEM imaging which reveal that CDAF Y contains a higher number of smaller conductive particles compared to larger flake-like fillers. The finer morphology of CDAF Y enhances the ability to conform to the complex topography of the mother die's active surface, thereby minimizing the occurrence of resin-rich regions or voids both of which can serve as initiation sites for delamination[3]. Furthermore, particle counts with Feret's diameters exceeding 100 µm were detected in CDAF X, supporting the noted disparity in particle morphology. However, such findings do not definitively indicate a lack of surface conformity as conductive fillers in

CDAF X were still observed in close proximity to the mother die's active surface.

4.6 Capacitance Measurement of Stacked Die Configurations Using the Two CDAF Materials

Through DC Test measurement, the capacitance (denoted by "Cap" test parameter) in Farad was measured to check efficiency of both CDAF materials to reduce the capacitance of the stacked capacitor dies.

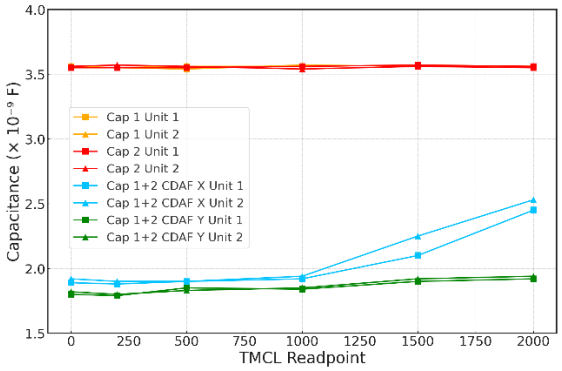

Fig. 13. Capacitance of Single and Stacked Die Using CDAF X (blue) and Y (green) Materials Across TMCL Readpoints.

Experimental results revealed a marked reduction in capacitance that is nearly 50% when a stacked die configuration was implemented for Capacitor 1 and Capacitor 2 relative to the baseline values obtained from single capacitor measurements. The comparison as illustrated by yellow and red markers and lines in Fig. 13, highlights the effect of die stacking on electrical behavior. Statistical analysis using Repeated Measures ANOVA confirmed a significant variation in capacitance between units assembled with CDAF X and Y. Among the two, CDAF Y exhibited significantly lower capacitance values in the initial measurement. Following 1500 thermal cycles, both CDAF materials showed an increase in capacitance. However, units assembled with CDAF Y maintained capacitance values substantially lower and more consistent with approximately half of the single capacitor reference. Such behavior indicates greater capacitance stability and suggests enhanced adhesion integrity of CDAF Y on the top active surface of the die. The higher stability of CDAF Y adhesion with top active side of the mother die likely contributes to superior electrical performance retention under prolonged thermal stress conditions.

4.7 Proposed Loop Height Design Rule for Stacked Die Configurations

As part of the development of a stacked-die architecture for overmolded packages, the loop height configuration must be appropriately defined to avoid potential wire bonding defects on the top die. A simplified schematic illustrating the stacked-die configuration, along with key dimensional parameters, is presented in Fig. 14.

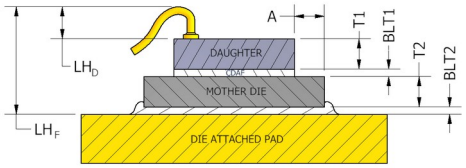

Fig. 14. Dimensional Illustration of Stacked Die Reference for Wirebond Design Rule.

T1 and T2 represent the daughter and mother die thicknesses, while BLT1 and BLT2 represent the bond line thicknesses of the CDAF and the die attach layer beneath the mother die, respectively. Margin A ensures a minimum 65 µm edge clearance between stacked dies and serves as a design reference. LHF defines the maximum allowable loop height from the heatsink or flange surface to avoid wire sweep, whereas LHD is the recommended loop height for the daughter die's wire bonds, governed by:

(Equation 1)

The equation constrains wire loop height to prevent wire sweep exceeding 15%. Using CDAF Y with average thickness 30 µm, the calculated LHD for the evaluated package is 780 µm.

5.0 CONCLUSION

The study pioneers the application of CDAFs in stacked-die RF power semiconductor packages, demonstrating the feasibility in addressing the thermal, electrical, and mechanical challenges of next-generation 3D packaging. Through a systematic evaluation of two CDAF candidates, key findings reveal that both materials exhibit adequate thermal stability, mechanical robustness, and process compatibility. CDAF Y showed better material responses and more stable reduced capacitance after extended thermal cycling, making it a more favorable option for high-reliability applications.
The successful integration of CDAF into a pyramid-stacked die configuration not only improves adhesion and interfacial integrity but also enables a novel approach to capacitance optimization within the package, reducing parasitic effects critical to high-frequency RF performance. The proposed loop height design rule further supports manufacturability and reliability in overmolded configurations. Collectively, the results establish CDAF as a promising material for stacked RF packaging, opening new pathways for

compact, efficient, and thermally stable semiconductor device architectures.

6.0 RECOMMENDATIONS

To further enhance the scope of the investigation, it is recommended that reliability assessments be extended to include additional stress conditions such as Highly Accelerated Temperature and Humidity Stress Tests (HAST) or biased humidity testing. Additional research is also encouraged to explore alternative CDAF materials with different filler compositions and resin formulations to assess how material properties influence both adhesion reliability and electrical performance stability.

7.0 ACKNOWLEDGMENT

The authors wish to extend their deepest appreciation to the engineers and technicians at the Backend Technologies Competence Center for their assistance in conducting the experiments, to Failure Analysis & Reliability Department for the execution and provision of necessary tools, tests and support in the experiment, and to the management team of Ampleon Phils. Inc. for their support, which was instrumental in facilitating this research.

8.0 REFERENCES

1. M. R. Marks et al., ***IEEE Trans. Compon. Packag. Manuf. Technol.***, *4(12).* **2014**. 2042-2057.

2. A. Unger et al., ***Proc. IMAPS 47th Int. Symp. Microelectron., 2014***, *2014.* **2014**. 289-294.

3. S. Fu et al., ***Compos. Part B Eng.***, *39(6).* **2008**. 933-961.

4. R. J. C. Carbas et al., ***J. Adhes.***, *90(1).* **2012**. 104-119.

5. P. Savolainen et al., ***Ansys***. **2022**. 1-7.

6. P. Krishnan et al., ***IEEE 36th Int. Electron. Manuf. Technol. Conf.***, *4(12).* **2015**. 1-3.

9.0 ABOUT THE AUTHORS

Marty Lorgino D. Pulutan received the B. S. degree in Applied Physics specializing in Materials Physics from University of the Philippines, Los Baños in 2017 and currently pursuing M. S. degree in Materials Science and Engineering by Research in Mapua University. He has published a total of 10 papers in peer-reviewed journals and international conference proceedings. He is currently a Senior Materials Development Engineer under Back End Technologies Department in Ampleon Philippines, Inc.

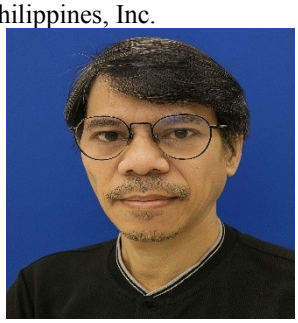

Norman Y. Lanuza received the B. S. Electronics and Communications Engineering in University of Sto. Tomas. He has 34 years of experience in semiconductor field particularly in equipment, process engineering and package development, and is currently a Principal Die Attach Engineer under Back End Technologies Department in Ampleon Philippines, Inc.

Patrisha Louise M. Reyes is a Jr. Project Management Engineer at AMPLEON Philippines Inc. since 2019. She graduated from Mapua University (For. M.I.T) – Intramuros, Manila where she earned a degree of Bachelor of Science in Manufacturing Engineering. Currently she is pursuing a degree of Master of Science in Management Engineering in Pangasinan State University – Urdaneta.

10.0 APPENDIX

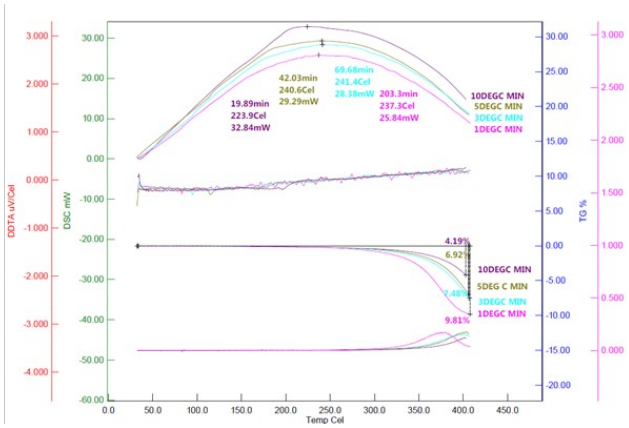

Fig. 15. DSC, TGA and Corresponding Derivative Curves of CDAF X Obtained at Heating Rates of 1, 3, 5, and 10 °C/min.

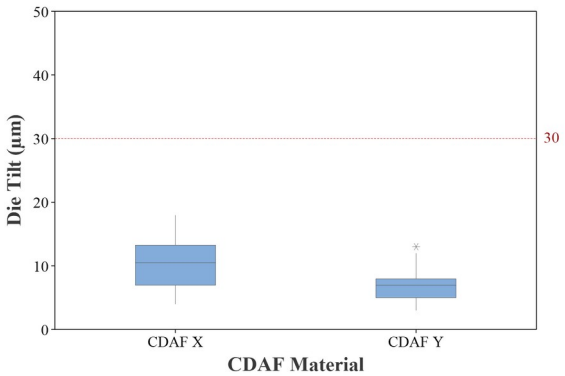

Fig. 16. Comparison of Die Tilt Measurements for CDAF X and Y.